SECM/13/240

FREE VIBRATION BEHAVIOUR OF FIBRECOMPOSITE SANDWICH BEAMS WITH DEBONDS

W. Karunasena[1], I. Jayathilake[2] and W. Lokuge[3]

[1]Centre of Excellence in Engineered Fibre Composites
School of Civil Engineering & Surveying
Faculty of Health, Engineering and Sciences, University of Southern Queensland,
Queensland, Australia
Telephone: 0061 7 4631 2906; Fax: 0061 7 4631 2526
E-mail: karu.karunasena@usq.edu.au

[2]Centre of Excellence in Engineered Fibre Composites
School of Civil Engineering & Surveying
Faculty of Health, Engineering and Sciences, University of Southern Queensland,
Queensland, Australia
Telephone: 0061 7 3470 2906
E-mail: Indunil.Jayatilake@usq.edu.au

[3]Centre of Excellence in Engineered Fibre Composites
School of Civil Engineering & Surveying
Faculty of Health, Engineering and Sciences, University of Southern Queensland,
Queensland, Australia
Telephone: 0061 7 3470 4477
E-mail: weena.lokuge@usq.edu.au

Abstract:

Although perfect bond between the skin and the core is a common assumption, an important issue that needs to be considered in using a composite beam or slab is the development of debonding between the skin and the core. Debonding refers to separation of skin from the core material in composite sandwiches. Although much research has been carried out to investigate dynamic behaviour of fully bonded composites, research on this aspect for debonded composites is scarce. This study concentrates on investigating the dynamic behaviour of fibre composite sandwich beams with debonds. A parametric investigation is carried out to assess the influence of various parameters of concern including length and width of the debond, location of debond, size and support conditions of the beam on the free vibration behaviour, using the finite element package Strand7. In the model developed with Strand7, rigid links and master slave links are used to connect skin and core in bonded and debonded regions respectively. Published results for free vibration behaviour for GFRP panels will first be used to compare the analytical results to validate the developed model. Furthermore a spring model is implemented between the skin and the core of debonded beams to take the probable contact conditions into account. A general reflection through the parametric investigation is that the extent of natural frequency variation with respect to debonding length increases with the order of the natural frequency. Further it is observed that the change in frequency with change in debonding length is much more significant for the full width debonding when

compared to half width debonding. It is also perceived that the extent of variation of natural frequency due to debonding in composite beams depends on the degree of contact anticipated in the debonding region.

Keywords: *Sandwich composite beams, Glass fibre-reinforced polymer, Dynamic behavior, Debonds, Finite element modeling*

1.0 Introduction

Fibre-reinforced polymer (FRP) composites are made up of a combination of fibres in a matrix material. A composite sandwich structure is fabricated by attaching two thin, stiff skins to a lightweight, high strength thick core which can serve as a building block for constructing laminated structural sandwich composites for building and other structural applications in civil engineering field. The main advantage of using the composite sandwich concept is that the resulting structure has high bending stiffness and high strength to weight ratio. In Australia, a new generation composite sandwich panel made up of glass fibre reinforced polymer skins and lightweight, high strength phenolic core material has been developed specifically for civil engineering applications (Van Erp, 2008) and their mechanical behaviour has been investigated thoroughly (Manalo *et al.*, 2010a and 2010b). Although the bending stiffness and strength of these composite panels can be controlled by changing the skin thickness and the core thickness, currently they are produced in limited thicknesses due to cost effectiveness and efficiency. Since its development, there has been an increased use of this fibre composite sandwich panel in structural applications such as floor slabs, pedestrian bridges and bridge decks. These structural components are manufactured from individual fibre composite sandwich panels or by gluing several layers of sandwich panels together to satisfy the strength and serviceability requirements. This paper focuses on applications involving individual sandwich panels or single layer panels.

The structural integrity of these panels can be severely affected by the skin-core debonding, which refers to separation of skin from the core materials. This debonding in sandwich structures has a very similar effect to that of delamination in laminated composite structures. Debonding could be due to manufacturing defects like incomplete wetting or entrapped air pockets in the adhesive layer between the core and skins. Debonding could also be caused by local separation of skin due to accidental dropping of tools during construction and maintenance of the composite structure (Burlayenko and Sadowski, 2010; Guedra, 1977). Water absorption, overloading and elevated temperature levels can also cause debonding (Manalo *et al.*, 2010c). Debonds are inherent potential cause for the structural failures in adhesively bonded composite structures (Abrate, 1997).

Debonding has an effect on the vibration parameters, such as natural frequencies and mode shapes of the beam. In particular, debonding could reduce the natural frequency and if the reduced natural frequency is close to the working frequency of the beam, resonance could happen, leading to serviceability issues related to deflection limits. Therefore, it is important to make accurate predictions of changes in natural frequencies in such structures. Moreover, having accurate predictions of changes of free vibration parameters is very useful for non-destructive detection of invisible defects such as debonding in sandwich construction.

The majority of research carried out so far has been concerned with delamination of laminated composite structures wherein very thin plys are laminated together to make up the structure. Skin-core

debonding in a fibre composite sandwich beam with thin composite faces (skins) and a thick core has received relatively minor attention. As the debonding of skin from the core in a composite sandwich beam is more or less analogous to split in an isotropic beam or delamination in a laminated composite structure, a review of literature in that area is appropriate. Reader is referred to recent articles by Lee (2000) and Della and Shu [2005, 2007) for a comprehensive review of literature in this area on investigation of delamination in laminated structures. Dynamic behaviour of sandwich plates containing skin/core debonding has been investigated by Burlayenko and Sadowski (2011). The free flexural vibration of an isotropic beam containing a full width delamination has been studied by several researchers using analytical, experimental and numerical methods in the past. Wang *et al.* (1982) presented an analytical model, referred to in the literature as 'free model' or 'unconstrained model' or 'without-contact model', consisting of four separate Euler-Bernoulli beam segments (to the left, right, above and below the delamination) joined together with appropriate boundary and continuity conditions. In their model, it was assumed that delaminated layers deform freely and have different transverse deformations. Although their numerical results were in reasonable agreement with experimental results, they included physically unreal overlapping at the delamination. Mujumdar and Suryanarayan (1988) presented 'the constrained model', which is also referred to as 'with-contact model' or simply 'contact model' in the literature. They assumed that delaminated segments of the beam are constrained to have same transverse displacements along the whole length of the beam but are free to slide over each other. Their analytical results were in excellent agreement with experimental results. This model was later extended by Shu and Fan (1996) for bi-material beams and Hu and Hwu (1995) for sandwich beams by including the effects of transverse shear deformations and rotary inertia. Similar analytical models were proposed by Tracey and Pardoen(1989) and Grouve*et al.*(2008) for laminated composite beams. However, these models exclude opening vibration modes found by Shen and Grady (1992). The models discussed so far, have been adapted by many researchers in different forms to study the behaviour of delaminated beams. Duggan and Ochoa (1992) suggested that the natural frequencies are sensitive to the size, location, and shape of delamination in structural components.

Modelling and detection of delamination in composites plates has been studied primarily with classical lamination theory (CLT) and first order shear deformation theory (FSDT) which is also known as Mindlin theory. The CLT completely ignores transverse shear deformations while FSDT accounts for them through shear correction factors. Ju*et al.* (1995) carried out a 2D finite element analysis based on the Mindlin theory to investigate the free vibration behaviour of delaminated composite plates. They found that mode shapes are not significantly affected but delamination effects on natural frequencies are mode dependent and some frequencies may be significantly affected.Qiao*et al.*(2007) used ANSYS finite element (FE) software to study the dynamic behaviour of delaminated composite beams. They used bi-linear contact elements with tension only option for modelling the delamination contact conditions. Lee (2000) used the layerwise theory to analyse the free vibration of delaminated composite beams. Chattopadhyay and Gu (1994) developed a refined higher order theory (HOT) which was shown to be accurate for delamination modelling in moderately thick composite plates. Later, Chattopadhyay *et al.* (2000) further extended this theory where HOT results were compared with experimental results and 3D finite element results using NASTRAN software package. Kim *et al.* [2003a, 2003b) presented an improved layerwise theory for dynamic analysis of delaminated composites. In their analysis, they used delaminated elements with additional nodal unknowns to model delamination effect.

Tenek *et. al.* (1993) studied the dynamic behaviour of delaminated composite plates using a 3D finite element method by assuming that the gap between delaminated layers is infinitely small. Kruger

(1999) presented a 3D shell modelling technique using Abaqus finite element software package for analysis of delaminated composite plates. Yam *et al.* (2004) proposed a 3D finite element analysis utilizing virtual elements in the region of delamination to prevent element penetration.

Chakrabarti and Sheikh (2009) carried out the dynamic analysis of a debonded sandwich plate by employing a linear spring model in the interfacial region. Kwon and Lannamann (2002) used a finite element analysis with surface-to-surface contact model to predict the dynamic behaviour of a debonded cantilever sandwich beam subjected to an impact load at the free edge. A high-order analytical approach for the free vibration analysis of fully bonded and debonded unidirectional sandwich panels with a transversely flexible core was presented by Schwarts *et. al.* (2008). In their approach, compressibility and shear deformability of the core, as well as 'with' and 'without' contact conditions at the debonding between skin and core were taken into account. Same authors (Schwarts et al. 2007) presented a modified Galerkin method to tackle the same problem. They verified their results against those from ANSYS FE analysis. Mendelsohn (2006) investigated the progressive failure of debonding in a sandwich plate by using the Dugdale-Barenblatt cohesive zone model. Recently, Burlayenko and Sadowski (2010) investigated the free vibration of sandwich plates with honeycomb and PVC foam cores containing single/multiple debonds between the core and the skin using a 3D finite element modelling approach. Using the Abaqus finite element software, they presented numerical results to show the influence of size, location and number of debonded zones on dynamic characteristics of sandwich plates. Senthil *et al.* (2013) did a comprehensive literature survey on the defects like debonds and delaminations in composite structures, and it was observed that though most commonly observed failure modes in composite structures are delamination and debonds, most studies were confined to delamination and little attention is paid to debond in adhesively bonded joints.

This paper presents a finite element method based numerical investigation of the effect of various amounts of debonding along the length and width of a beam on its natural frequency. Small test beams are first used to model and analyze the free vibration behaviour, and then these test specimen sizes are extended to a practical size. The commercial finite element software package Strand7 (2010) is used for modelling by giving due consideration to bonded and unbonded interfaces between skin and core using rigid and master-slave link elements as appropriate. Numerical FE model is verified by comparing with published results for a known problem. The verified model is used to investigate the variation of natural frequency with debonding length and width for beams with different boundary conditions such as simply supported, clamped-clamped and clamped-free. A spring model is implemented between the skin and the core of debonded single layer beams to take into account the probable contact conditions by varying the degree of contact between the two interfaces, allowing for a more realistic modelling of the debonded and delaminated structures' dynamic response. A comparison of contact and free models is presented with the aid of the application of a spring element in Strand 7.

2.0 Problem definition

In this research, a composite sandwich plate with core bounded by top and bottom skins with a finite debonding between the top skin and the core is considered (Figure 1).

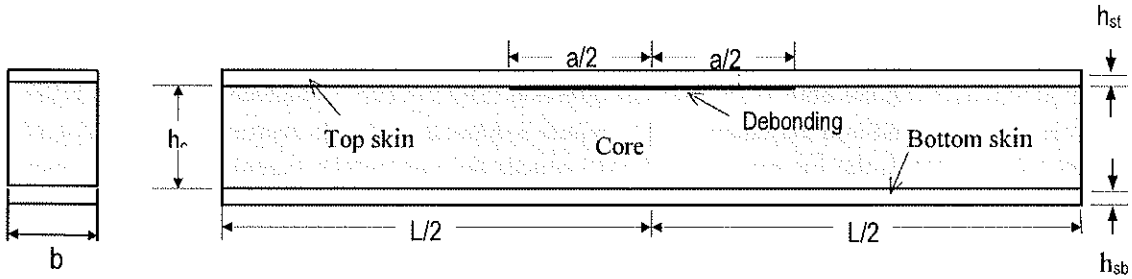

Figure 1: Longitudinal and cross sections of the sandwich beam with a central debondin

The geometric dimensions of the test beam and the full scale beam, the debonding length and location are as defined in Figure 1 and detailed in section 4.2. The beam cross-section is rectangular with a width of b. Materials in each of the skins is assumed to be homogeneous orthotropic and linear elastic. It is possible to have different materials for top and bottom skins. Core material is assumed to be linear elastic and homogeneous isotropic. Debonding is assumed to be an artificial flaw of zero thickness, embedded between top skin and core. It is assumed that debonding exists before vibration commences and stays constant without propagation during the vibration. Initially, debonded surfaces (of skin and core) are assumed to be in contact vertically but can slide in the horizontal plane. Later on, a spring damper element in Strand7 is used to simulate the 'constrained' or 'contact' models and 'free' models discussed in section 1, in order to compare the natural frequency responses for contact and free models.

3.0 Numerical model

Firstly, the FE model for the intact beam is described because the model for the debonded beam entails only a minor change to the intact beam model. The numerical modelling in this study is carried out using the 'natural frequency' solver in the Strand7 FE software package (2010). Linear elastic orthotropic top and bottom skins are modelled using 4-noded rectangular (Quad4) plate elements. The plate element mesh for each skin lies at the horizontal plane at the mid-thickness level of the respective skin. Core is modelled using linear elastic orthotropic 3D brick elements (Hexa8). These elements take care of any shear deformations happening in the thick core. It is noted that skins can be modelled using higher order plate elements such as 8-noded or 9-noded elements. In that case, core needs to be modelled with corresponding higher order elements to ensure compatibility (or alternatively, a special type of link elements in Strand7 can be used to force compatibility between higher order plate elements and linear core elements). However, in this study, for simplicity, Quad4 and Hexa8 linear elements are used for skins and core, respectively. Core 3D FE mesh is generated by extruding the Qaud4 plate element mesh using the 'extrude' command in strand7. This ensures that a vertical line through corresponding plate nodes in the top and bottom skins will pass through corresponding brick nodes in the core. The structural integrity between top skin and core is assured by connecting plate nodes with corresponding brick nodes at the top surface level of the core through vertical 'rigid link' elements. These links are of length $h_{st}/2$ where h_{st} is the thickness of the top skin as shown in Figure 1. These rigid links ensure that there is no gap or sliding between the top skin and the core. In a similar manner, bottom skin is connected to the bottom surface of the core using rigid links of length $h_{sb}/2$ where h_{sb} is the thickness of the bottom skin.

The FE model for the debonded beam can be obtained by simply converting the rigid links within the debonded region to 'master slave links' in Strand7 with appropriate degrees of freedoms. These links will allow for sliding between interfaces of skin and core in the horizontal directions while keeping skins in contact with the core in the vertical direction. This process effectively embeds an artificial zero thickness debond into the intact plate to mimic a debonded plate to represent the constrained or contact model. After the FE model has been created, the appropriate eigenvalue problem can be solved to obtain natural frequencies and corresponding mode shapes.This scenario is analogous to contact model state. As usual in the conventional finite element method, more elements will ensure better convergence and, therefore, appropriate numerical studies are carried out to get a reasonably converged solution.

Next, a spring model is implemented between the skin and the core of debonded single layer beams by removing the master slave links and replacing them with spring damper elements in Strand7 to facilitate the investigation of the influence of degree of contact on the natural frequency. Firstly the axial stiffness of the spring was increased until the analyses give similar frequency values as accomplished for the constrained model with master-slave links described above. Then a free model is simulated by assigning zero stiffness for these spring elements.
Finally, a full scale composite beam with dimensions given in section 4.2 is analyzed and prominent results are presented for comparison with the test beam.

4.0 Results and discussion

The numerical model described in the previous section was used to obtain natural frequencies for a variety of sandwich beams. Firstly, the numerical model is verified by comparing model results with those reported in the literature for a known problem. Thereafter, numerical results for natural frequencies of the new generation sandwich composite beams described in section 4.2 are presented.

4.1 FE Model verification

To verify the accuracy of the results from the model used in this study, the natural frequencies from the proposed model for a foam core sandwich beam are computed and compared with results reported by Burlayenko and Sadowski (2011) and Schwarts *et al.* (2007). The debonding considered in these studies is centrally located at the interface between top skin and core, extending through the full width b of the beam. Figure 1 shows a longitudinal section of the beam and the dimensions used are L = 300 mm, b = 20 mm, a = 20 mm, h_c = 19.05 mm, h_{sb} = 1 mm and h_{st} = 0.5 mm. Natural frequencies of intact and debonded beams were obtained by Burlayenko and Sadowski (2011) using Abaqus FE code and by Schwarts et al. (2008) using a higher order analytical approach.
The beam is simply supported at the ends of both top & bottom skins.Material properties of the beam are given in Table 1.

Table 1: Material properties of foam core sandwich beam (verification problem)

Property	Skins	Core
Type	Isotropic	Isotropic
Young's modulus, E (MPa)	36000	50
Poisson's ratio, ν	0.3	0.19
Density, ρ (kg/m^3)	4400	52

A convergence study was carried out by suitably refining the FE mesh to obtain natural frequencies as accurately as possible with the minimum number of elements to save computational effort. The finally accepted FE mesh consists of 11979 nodes with 1920 plates (8x120 in each of the skins), 7680 bricks (8x8x120 in the core) and 2178 links (2x9x121 from plate nodes to top and bottom surface nodes in the core).

A comparison of the numerical results of the first five bending natural frequencies from the proposed study with those from literature (Burlayenko and Sadowski, 2011; Schwarts et al. 2007) is presented in Table 2 and Table 3. Table 2 is for the intact plate whereas Table 3 is for the debonded plate. It can be seen that current Strand7 results are in reasonable agreement with the results reported in the literature.

Table 2: First five bending natural frequencies (Hz) of intact foam core sandwich plate

Mode	This research		Abaqus (Burlayenko and Sadowski, 2011)	ANSYS (Schwarts *et al.* 2007)	Modified Galerkin Method (Schwarts *et al.* 2007)
	Coarse Mesh	Fine Mesh			
1	293.46	293.52	293.46	290.76	289.18
2	722.63	722.96	707.09	710.67	708.29
3	1138.60	1139.51	1106.70	1117.70	1114.24
4	1543.93	1545.91	1495.80	1515.30	1511.14
5	1863.50	1863.62	1818.70	1907.09	1902.25

Table 3: First ten natural frequencies (Hz) of debonded foam core sandwich plate

Mode	This research		Abaqus (Burlayenko and Sadowski, 2011)
	Coarse Mesh	Fine Mesh	
B1	293.46	293.52	293.07
L1	361.04	360.81	433.67
T1	534.39	540.79	-[b]
B2	712.39	710.75	-[b]
B3	1138.47	1139.31	1093.2
T2	1142.50	1146.32	1132.0
T3	1385.59	1394.31	-[b]
B4	1520.84	1520.84	-[b]
B5	1861.90	1861.72	1769.9
B6	1945.08	1948.35	1948.35

b – Not reported in reference (Burlayenko and Sadowski, 2011)

B – Bending mode; L – Lateral mode; and T – Twisting mode

4.2 Numerical results for the novel composite sandwich beam

Free vibration frequencies for the first five modes for the novel composite sandwich beam with full width, half width and various lengths of debonding along the length of the beam are presented in this section. Three boundary conditions, namely, both ends simply supported (S-S), clamped-clamped (C-C) and clamped-free (C-F) are used in the analysis. The relevant dimensions for the novel composite sandwich beam are (see Figure 1):

(a) For the test beam

L = 300 mm, b = 20 mm, h_c = 16 mm and $h_{sb} = h_{st}$ = 2 mm.

(b) For the full scale beam

L = 3m, b = 20 cm, h_c = 16 cm and $h_{sb} = h_{st}$ = 2 cm.

Debonding length 'a' varies from

(a) 30 mm to 270 mm in steps of 30 mm for the test beam model, and

(b) 30 cm to 270 cm in steps of 30 cm for the full scale beam model

The debonding is located centrally along the length of the beam and extends through the full width of the beam for case 1, and only middle half width for case 2. Each beam presented here is a new generation sandwich composite structure mentioned in the introduction of this paper and consists of a rigid core bonded to the top and bottom glass fibre composite skins. More information on this sandwich structure is stated in the literature (Van Erp, 2008; Manalo *et al.*, 2010a; 2010b; 2010c). The effective mechanical properties used in this study for the fibre composite skin and the core material of the sandwich beam are listed in Table 4. In the analysis, the skin is assumed as orthotropic while the core is assumed as an isotropic material.

Table 4: Effective mechanical properties and thicknesses of fibre composite skin and corematerial

Property	Skin	Core
Young's modulus along long direction (MPa)	15380	1150
Young's modulus in transverse direction (MPa)	12631	1150
Poisson's ratio	0.25	0.30
Density (kg/m^3)	1366	855

Typical 3D finite element models created with Strand7 for the beams with C-F, S-S and C-C end conditions are shown in Figure 2.

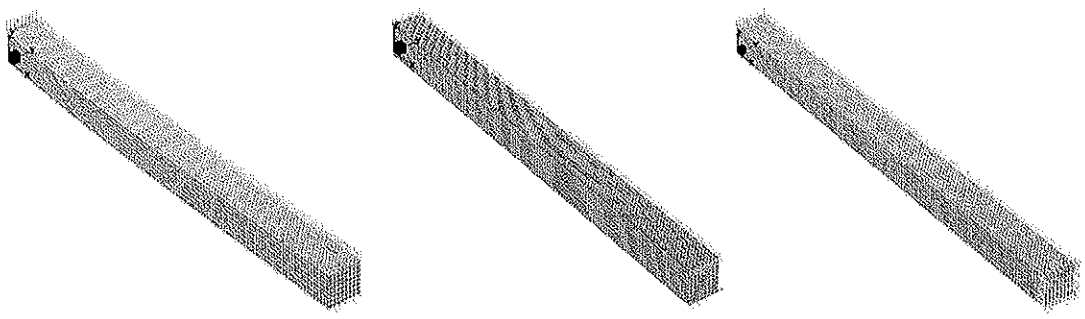

(a) (b) (c)

Figure 2: Typical 3D Finite element models of beams with Strand7

(a) C-F beam (fully bonded)

(b) S-S beam 30mm debond length (full width debonding)
(c) C-C beam 150mm debond length (half width debonding)

Frequency results for case 1 for the test beam are listed in Table 5, 6 and 7. Table 5 presents results for a beam with simply supported (S-S) ends while Tables 6 and 7 shows results for C-C and C-F end conditions, respectively. Similarly, Tables 8, 9 and 10 illustrate case 2 results for half width debonding. It is observed that, in general, the extent of natural frequency variation with respect to debonding length increases with the order of the natural frequency, giving the least variation forthefirst frequency. The results for the two cases indicate that the natural frequency response is significantly affected by full width debonding whereas half width debonding has only a slight influence on natural frequencies.

Table 5: First five bending frequencies (in Hz) of a simply-supported (S-S) novel sandwich beam with through-width debond

Debond length, a/L	Mode 1	Mode 2	Mode 3	Mode 4	Mode 5
0	289.78	1015.26	1580.87	2103.39	3152.96
0.1	289.78	1004.14	1577.27	2102.16	3068.59
0.2	289.72	954.04	1561.91	2085.11	2818.74
0.3	289.43	864.98	1537.75	2011.43	2660.67
0.4	288.48	768.90	1505.78	1866.39	2636.19
0.5	286.15	689.94	1442.13	1737.26	2610.09
0.6	281.56	633.54	1347.37	1686.34	2477.64
0.7	273.87	597.35	1270.42	1675.93	2288.38
0.8	262.72	577.46	1230.09	1666.79	2137.18
0.9	247.91	569.99	1218.40	1629.04	2062.35

Table 6: First five bending frequencies (in Hz) of a clamped- clamped (C-C) novel sandwich beam with through-width debond

Debond length, a/L	Mode 1	Mode 2	Mode 3	Mode 4	Mode 5
0	592.28	1421.21	2440.31	3535.90	3559.82
0.1	592.25	1401.74	2438.94	3444.76	3537.24
0.2	591.71	1320.98	2413.64	3138.73	3537.09
0.3	588.71	1203.55	2301.44	2974.30	3533.40
0.4	579.16	1110.95	2097.59	2954.38	3501.87
0.5	557.67	1065.27	1916.46	2920.99	3395.82
0.6	521.33	1055.28	1826.33	2776.32	3288.57
0.7	473.15	1051.72	1810.52	2629.06	3227.69
0.8	420.10	1018.48	1795.04	2586.58	3152.76
0.9	368.58	942.71	1706.80	2563.78	3044.52

Table 7: First five bending frequencies (in Hz) of a clamped- free (C-F) novel sandwich beam with full-width debond

Debond length, a/L	Mode 1	Mode 2	Mode 3	Mode 4	Mode 5
0	106.69	609.16	1517.53	1772.36	2609.95
0.1	106.57	609.09	1492.06	1772.05	2603.27
0.2	105.95	608.36	1386.67	1771.12	2553.26
0.3	104.48	604.98	1234.81	1770.03	2407.51
0.4	101.95	595.15	1110.89	1768.60	2174.50
0.5	98.31	574.55	1038.25	1765.15	1972.93
0.6	93.73	541.74	1007.44	1755.18	1870.65
0.7	88.51	500.08	999.21	1735.34	1848.44
0.8	82.97	455.31	991.19	1703.66	1840.11
0.9	77.42	412.31	965.71	1659.41	1794.04

Table 8: First five bending frequencies (in Hz) of a simply-supported (S-S) novel sandwich beam with half-width debond

Debond length, a/L	Mode 1	Mode 2	Mode 3	Mode 4	Mode 5
0	289.78	1015.26	1580.87	2103.39	3152.96
0.1	289.78	1013.84	1580.40	2103.13	3142.35
0.2	289.77	1012.07	1579.71	2100.98	3133.75
0.3	289.75	1010.81	1578.96	2095.76	3132.53
0.4	289.70	1010.16	1578.14	2088.93	3130.09
0.5	289.62	1009.97	1577.27	2083.35	3119.68
0.6	289.51	1009.94	1576.38	2080.78	3105.48
0.7	289.37	1009.70	1575.51	2080.43	3096.71
0.8	289.20	1008.95	1574.64	2079.41	3095.27
0.9	288.98	1007.32	1573.77	2074.04	3091.62

Table 9: First five bending frequencies (in Hz) of a clamped- clamped (C-C) novel sandwich beam with half-width debond

Debond length, a/L	Mode 1	Mode 2	Mode 3	Mode 4	Mode 5
0	592.28	1421.21	2440.31	3535.90	3559.82
0.1	592.27	1418.73	2439.96	3534.49	3546.90
0.2	592.19	1415.88	2436.47	3529.26	3541.22
0.3	591.95	1414.32	2428.36	3527.88	3540.82
0.4	591.47	1413.94	2418.92	3526.55	3536.15
0.5	590.72	1413.85	2412.84	3514.43	3532.35
0.6	589.71	1412.84	2411.36	3499.77	3531.80
0.7	588.47	1409.90	2410.77	3495.16	3531.59
0.8	587.06	1404.69	2405.30	3493.64	3531.38
0.9	585.56	1397.65	2392.18	3479.51	3531.26

Table 10: First five bending frequencies (in Hz) of a clamped-free (C-F) novel sandwich beam with half-width debond

Debond length, a/L	Mode 1	Mode 2	Mode 3	Mode 4	Mode 5
0	106.69	609.16	1517.53	1772.36	2609.95
0.1	106.68	609.15	1514.29	1772.32	2608.90
0.2	106.65	609.07	1510.53	1772.26	2603.95
0.3	106.63	608.85	1508.41	1772.20	2593.81
0.4	106.61	608.42	1507.80	1772.15	2582.62
0.5	106.59	607.78	1507.72	1772.09	2575.68
0.6	106.57	606.96	1506.90	1772.03	2573.93
0.7	106.55	606.00	1504.48	1771.96	2573.19
0.8	106.53	604.99	1500.43	1771.90	2568.32
0.9	106.51	603.98	1495.48	1771.84	2558.35

A normalized form of the frequency results of first three frequencies for full width debonding with regard to the three end conditions considered are shown in Figure 3.

Note here that ω is the frequency of the virgin plate for the corresponding mode. Comparison of frequency variations for the three end conditions illustrated in Figure 3 reveals that first natural frequency has the least effect on debonding for the case of full width debonding. Careful observation of Tables 8, 9 and 10 further reveals that this is true for half width debonding as well. It is interesting to note from Figure 3 that debonding does not have much effect on the first frequency when delamination length, a/L, is less than 0.4 for all three end conditions considered in the analysis. In fact, second mode frequency is the most sensitive frequency to debonding length for both S-S and C-C end conditions, with the only exception occurring at C-C beam which shows a sharp drop for first natural frequency for debonding length of 0.9L, giving it the least value out of the three modes. On the contrary, for C-F beam, third mode dominates with regard to sensitivity to debonding length. In addition, mode 1 and 2 frequencies of the C-F beam show nearly the same sensitivity to debonding length in contrast to the vast difference shown by S-S and C-C beams for the same. This is an interesting observation which reveals that the end conditions of the beam is a governing factor dictating which modes are more affected. It is also interesting to observe that the first natural frequency is unaffected when a/L is less than 0.3 for all three end conditions. Further, it is seen that the maximum reduction in natural frequencies is around 50% of fully bonded beam frequencies for both simply supported and clamped-clamped end conditions when the debonding is right through the full length of the composite beam. This is of great importance as this confirms that if the working frequency of the beam is kept away from the range 50% to 100%, it is very unlikely that resonance would occur for the test beam considered.

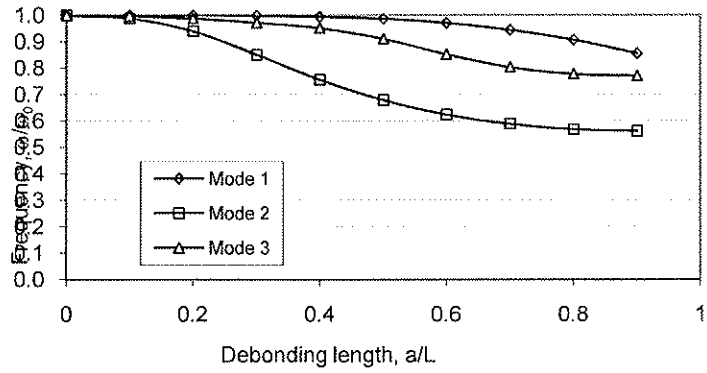

(a) S-S beam

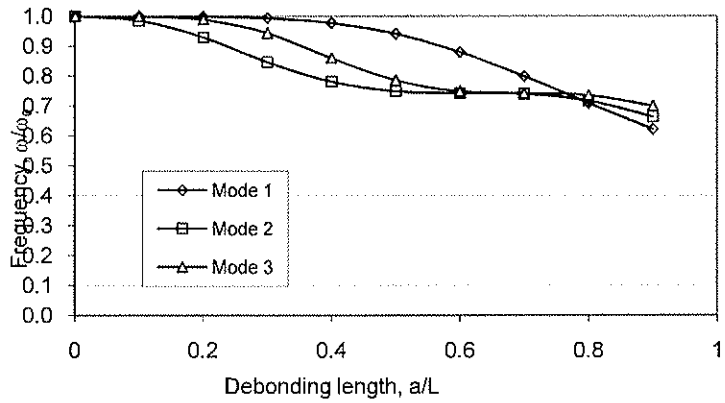

(b) C-C beam

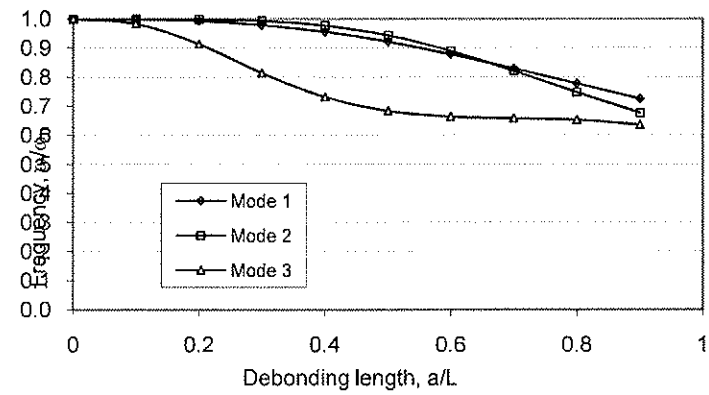

(c) C-F beam

Figure 3: Comparison of frequency variation ω/ω_0 with debonding length for the composite beam with full width debonding for (a) S-S, (b) C-C and (c) C-F end conditions

In models with spring elements assigned in place of master slave link elements, it was observed that, the frequency results give similar values as expected for similar debonding with master slave links,

when the axial stiffness is increased to 1000 N/mm. Note here that the results are not included due to limitation of pages. Thus it is revealed that spring elements can successfully be accommodated to model the required degree of contact in debonding region, by assigning the appropriate stiffness for the spring element. This is specifically important in simulating partial debonding, which will be investigated in future.

Figure 4 shows the comparison of natural frequencies for constrained (contact) and free models for the test beam for 30 mm debonding length with half width and full width debonding for C-C case. It is clearly observed that the variation in natural frequency for contact and free models are much more significant for full width debonding than half width debonding. Further it is revealed that this variation is negligible for lower mode numbers and becomes significant for higher mode numbers, but not necessarily in the increasing order of the mode numbers. For example, Figure 4(b) reveals that the frequency variation is more significant for mode 8 than for mode 9. The same trend is seen for other cases and other debonding lengths as well.

Figure 5 demonstrates the comparison of natural frequencies for constrained (contact) and free models for the test beam for 270 mm debonding length with half width and full width debonding for C-C case. It is interesting to observe that there is a significant variation of natural frequency for contact and free models in 270 mm full width debonding, compared to 30 mm full width debonding. It can, therefore, be concluded that both width and length of debonding will greatly influence the extent of natural frequency variation between contact and free models. In addition it is also clear that full width debonding has much more pronounced effect on this variation than half width debonding, revealed by the vast discrepancy in frequency seen in contact and free models in 270mm full width debonding case illustrated in Figure 5.

The comparison for the similar case discussed above for the full scale beam having 270 cm debonding is shown in Figure 6. Note here that the full scale beam represents ten times the size of the test beam. As expected, a similar trend is observed with full scale beam, compared to test beam results discussed above for 270 mm debonding. This in fact is a stimulating observation revealing the importance of choosing the proper degree of contact in debonding region in the analysis of debonded composite beams used in practice.

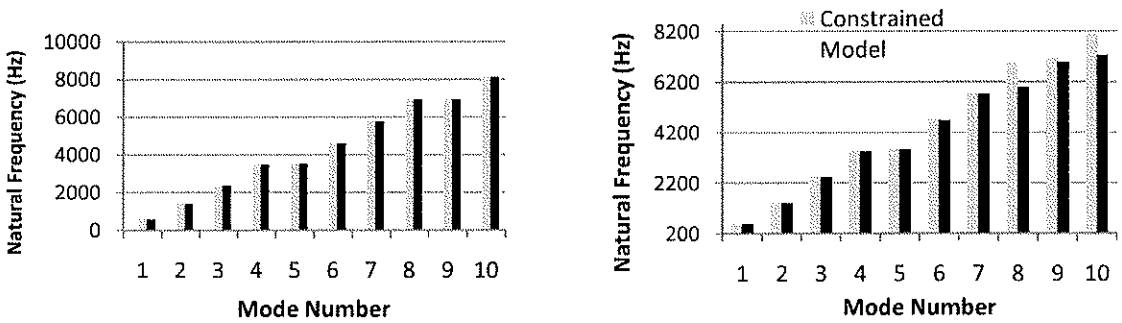

(b)

Figure 4: Comparison of natural frequencies for constrained and free models for test beam

(a) 30mm half width debonding for C-C case

(b) 30mm full width debonding for C-C case

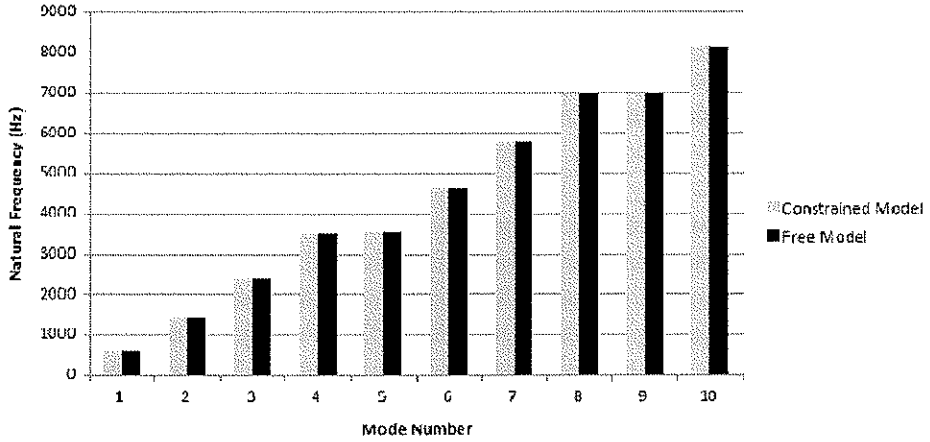

(a)

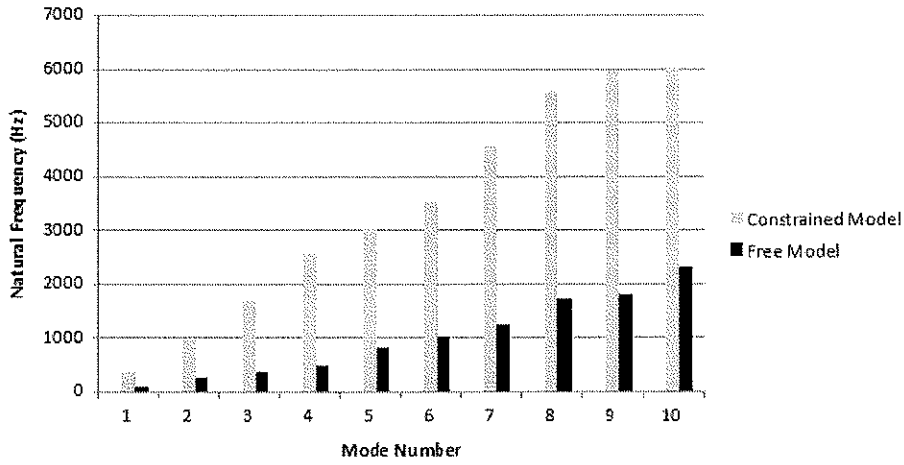

(b)

Figure 5: Comparison of natural frequencies for constrained and free models for test beam

(a) 270 mm half width debondingfor C-C case

(b) 270 mm full width debonding for C-C case

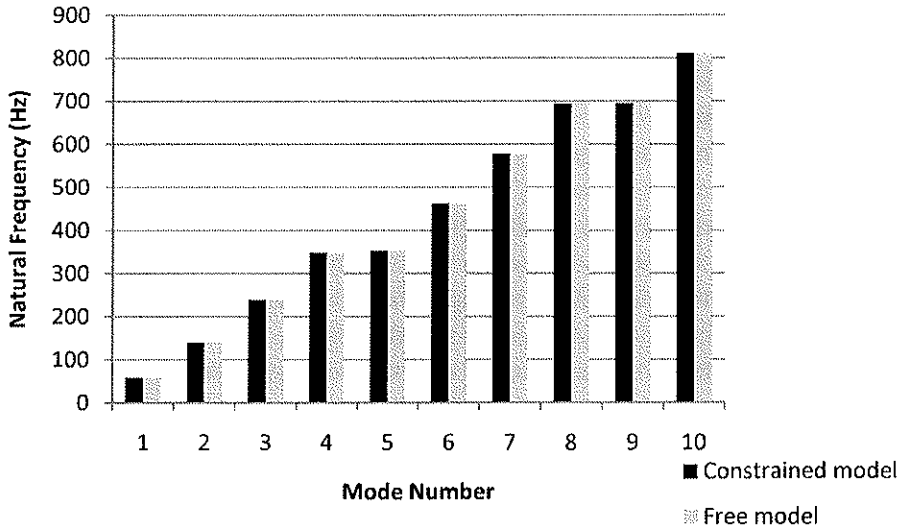

(a)

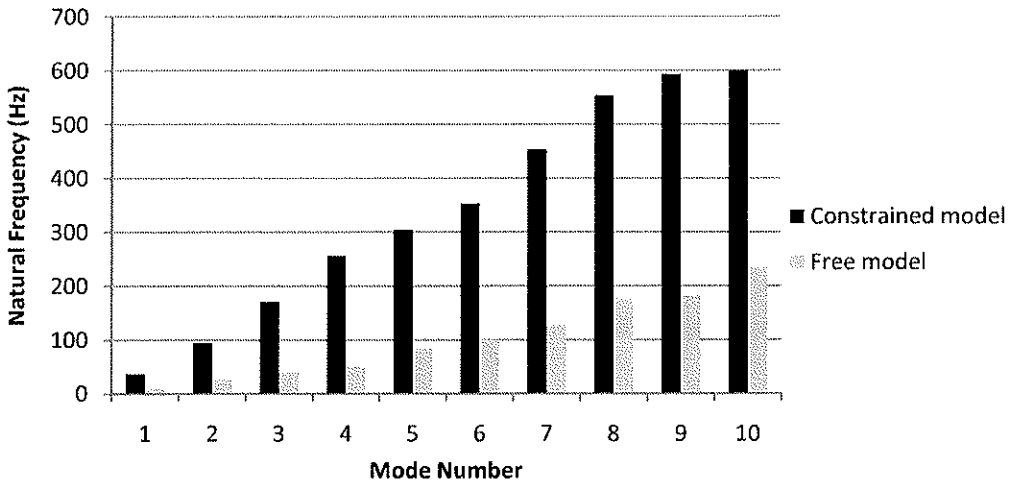

(b)

Figure 6. Comparison of natural frequencies for constrained and free models for full scale beam

(a) 270 cm half width debonding for C-C case

(b) 270 cm full width debonding for C-C case

5.0 Conclusions

This paper presents a numerical investigation into changes in natural frequency due to various amounts of debonding along the length and width of a composite test beam for simply supported, clamped-clamped and clamped-free boundary conditions. Prominent results for a full scale beam are also included for comparison. The numerical analysis was carried out by innovatively using plate and link elements (rigid links and master slave links) in Strand7 finite element software package. Three dimensional models of the beams were created for the analyses for more realistic assessment of the free vibration behaviour. The accuracy of the numerical solution was verified by comparing present results with reported results from the literature. Based on the results of the analyses, the following

conclusions are made.

I. Generally, debonding causes reduction in natural frequency when compared with fully bonded composite beams.
II. The extent of natural frequency variation with respect to debonding length increases with the order of the natural frequency, giving the least variation for the first frequency. The natural frequency decreases more rapidly as the mode number increases.
III. The decrease in natural frequency with the increase in the extent of debonding is more dependent on the width of debonding across the beam than the length along the beam for the novel composite beam considered in the analysis.
IV. The end conditions of the beam are also a governing factor dictating which modes are more affected.
V. If the working frequency of the beam is kept away from the range 50% to 100% of the virgin beam, there won't be resonance happening due to debonding in the test beam considered in the analysis.
VI. The extent of variation of natural frequency due to debonding in composite beams highly depends on the degree of contact anticipated in the debonding region.
VII. The natural frequency reduction due to debonding is higher for the free model compared to the constrained model for similar conditions of debonding. This discrepancy becomes more pronounced for full width debonding compared to half width debonding in the test beam considered. This is the case for both test beam and full scale beam scenarios.

References

Abrate, S. (1997): "Localized impact on sandwich structures with laminated facings",*Applied Mechanics Review*,**50,** pp.62–82

Burlayenko, V.N. and Sadowski, T. (2010): "Influence of skin/core debonding on free vibration behaviour of foam and honeycomb cored sandwich plates",*Int. Journal of Non-Linear Mechanics*,**45**, pp. 959-968.

Burlayenko, V.N. andSadowski. T. (2011): "Dynamic behaviour of sandwich plates containing single/multiple debonding", *Computational Materials Science***50**, pp.1263-1268.

Chakrabarti, A. and Sheikh, A.H. (2009): "Vibration and Buckling of Sandwich Laminates having Interfacial Imperfections",*Journal of sandwich structure and materials***11**, pp. 313–328.

Chattopadhyay, A. andGu, H. (1994): "A new higher order plate theory in modelling delamination buckling of composite laminates", *AIAA Journal* **32(8)**, pp. 1709-1718.

Chattopadhyay A, Radu, A.G. andDragomir-Daescu, D. (2000): "A higher order plate theory for dynamic stability analysis of delaminated composite plates", *Computational Mechanics*, **26**, pp.302-308.

Degeorges, D., Thevenet, P.and Maison, S. (1977): Damage tolerance of sandwich structures, in: Proceedings of Euromech 360 Colloquium, Kluwer Academic Publishers, Saint Etienne, pp. 29–36.

Della, C.N. and Shu, D. (2005): "Vibration of beams with double delaminations",*Journal of Sound and Vibration*, **282**, pp. 919-935.

Della, C.N. andShu, D. (2007):"Free vibration analysis of delaminated bimaterial beams",*Composite Structures*, **80**, pp. 212-220.

Duggan, M. and Ochoa, O. (1992):"Natural frequency behaviour of damaged composite materials",*Sound and Vibration*, **158**, pp. 545-551.

Grouve, W.J.B.,Warnet, L., De Boer, A., Akkerman, R. and Vlekken, J. (2008):"Delamination detection with fibre bragg gratings based on dynamic behaviour", *Composite Science and Technology*, **68**, pp. 2418-2424.

Hu, J.S. andHwu, C. (1995):"Free vibration of delaminated composite sandwich beams",*AIAA Journal*, **33(10)**, pp. 1911-1918.

Ju, F., Lee, H.P. and Lee, K.H. (1995):"Free vibration of composite plates with delamination around cutouts", Composite Structures 1995; **31**, pp.177–183.

Kim, H.S., Chattopadhyay, A. andGhoshal, A. (2003a):"Dynamic analysis of composite laminates with multiple delamination using improved layerwise theory",*AIAA Journal*, 41(9), pp. 1771-1778.

Kim, H.S., Chattopadhyay, A. andGhoshal, A. (2003b):"Characterisation of delamination effect on composite laminates using a newgeneralisedlayerwise approach",*Computers and Structures*, **81**, pp. 1555-1566.

Krueger, R. and shell, A. (1999):"3D modeling technique for delaminations in composite laminates".In: *Proceedings of American Society of Composites*, pp. 843–852.

Kwon, Y.W. andLannamann, D.L. (2002):"Dynamic Numerical Modelng and simulation of Intefacial Cracks in Sandwich Structures for damage detection"*J. Sandwich Struct. & Mater*, **4 (2)**, pp.175–199

Lee, J. (2000):"Free vibration analysis of delaminated composite beams",*Computers and Structures***74**, pp.121-129.

Manalo, A.C., Aravinthan, T., Karunasena W. and Islam, M.M. (2010a):"Flexural behaviour of structural fibre composite sandwich beams in flatwise and edgewise positions",*Composite Structures*,**92(4)**, pp. 984-995.

Manalo, A.C., Aravinthan, T. and Karunasena, W. (2010b):"Flexural behaviour of glue-laminated fibre composite sandwich beams",*Composite Structures*, **92(11)**, pp. 2703-2711.

Manalo AC, Aravinthan T, Karunasena W.(2010c):"In-plane shear behaviour of fibre composite sandwich beams using asymmetrical beam shear test",*Construction and Building Materials* **24(10)**, pp. 1952-1960.

Mendelsohn, D.A. (2006): "Free vibration of an edge-cracked beam with a Dugdale–Barenblatt cohesive zone",*J. Sound Vibration*, **292**, pp. 59–81.

Mujumdar, P.M. andSuyanarayan, S. (1988): "Flexural vibration of beams with delamination", *Journal of Sound and Vibration*, **125**, pp. 441-461.

Qiao, P., Lestari, W., Shah, M.G. and Wang, J. (2007):"Dynamics-based Damage Detection of Composite Laminated Beams using Contact and Noncontact Measurement Systems".*Journal of CompositeMaterals*, **41 (10)**, pp. 1217–1252.

Schwarts, G.H., Rabinovich, O. and Frostig, Y. (2008): "Free vibration of delaminated unidirectional sandwich panels with a transversely flexible core and general boundary conditions - A high-order approach" *J. Sandwich Struct. Mater.* 10, pp. 99-131.

Schwarts,G.H., Rabinovich, O. and Frostig, Y. (2007): "Free vibrations of delaminated unidirectional sandwich panels with a transversely flexible core-a modified Galerkinapproach",*Journal of Sound and Vibration*, **301**, pp. 253-277

Senthil, K., Arockiarajan, A., Palaninathan, R., Santhosh, B. andUsha, K.M.(2013): "Defects in composite structures: Its effects and prediction methods –A comprehensive review", *Composite Structures*,**106**, pp. 139–149

Shen, M.H. and Grady, J.E. (1992):"Free vibration of delaminated beams", *AIAA Journal*, **30(5)**, pp. 1361-1370.

Shu, D. and Fan, H. (1996): "Free vibration of a bimaterial split beam",*Composites: Part B*, **127(1)**, pp. 79-84.

Strand7. (2010):"Strand7 finite element analysis FEA software, Release 2.4.1", Sydney, Australia (website: www.strand7.com).

Tenek, L.H., Henneke, E.G. and Gunzbhurger, M.D. (1993) "Vibration of delaminated composite plates and some applications to non-destructive testing",*Composite Structures*, **23 (3)**: pp. 253–262

Tracey, J.J. andPardoen, G.C. (1989):"Effect of delamination on the natural frequencies of composite laminates",*Journal of Composite Materials*, **23(12)**, pp.1200-1215.

Van Erp, G. and Rogers, D. (2008):"A highly sustainable fibre composite building panel", In: *Proceedings of the International Workshop on Fibre Composites in Civil Infrastructure – Past, Present and Future*, University of Southern Queensland, Toowoomba, Queensland, Australia, 1-2 December 2008. Pp. 17-23

Wang, J.T.S., Liu, Y.Y. andGibby, J.A. (1982):"Vibration of split plates", *Journal of Sound and Vibration*,**84**, pp. 491-502.

Yam, L.H., Wie, Z., Cheng, Z. and Wong, W.O. (2004):"Numerical analysis of multi-layer composite plates with internal delamination",*Computers and Structures*, **282**, pp. 627–637.